Radiation from relativistic jets associated with black holes

Ioana Duțan

Institute of Space Science (ISS), Bucharest-Măgurele, Romania

work with:
K.-I. Nishikawa, A. Meli, C. Köhn, N. MacDonald,
Y. Mizuno, O. Kobzar, J. Gómez, K. Hirotani

Outline

Outline

Outline

Relativistic jets in active galactic nuclei (AGN)

- supermassive spinning black hole ($M \sim 10^7 - 10^9\, M_\odot$)
- surrounded by an accretion disk
- relativistic plasma jets: $v_{\rm jets} \sim 0.9 - 0.995\, c$
- Lorentz factor: $\Gamma \sim 2 - 10$
- $\Gamma = \beta\gamma_0$, with $\beta = v/c$ and $\gamma_0 = (1-\beta^2)^{-1/2}$

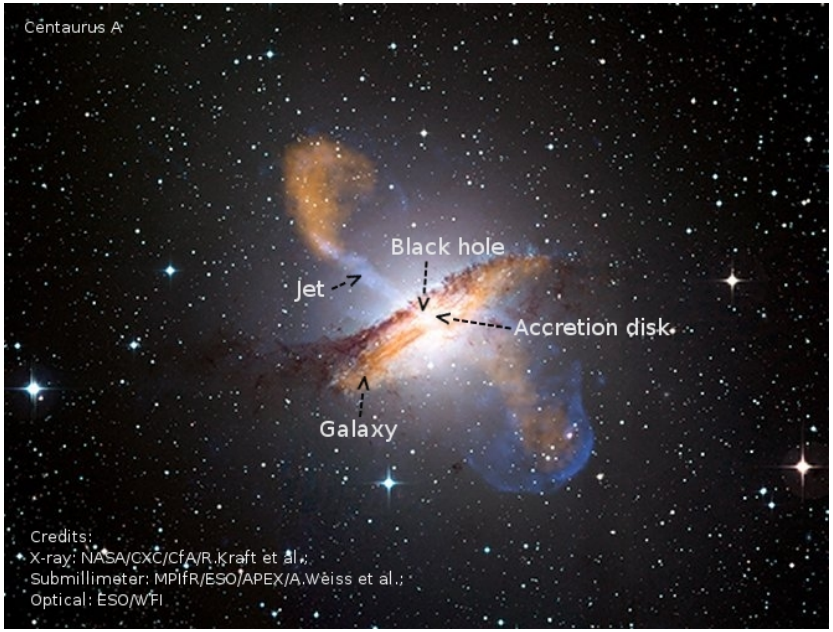

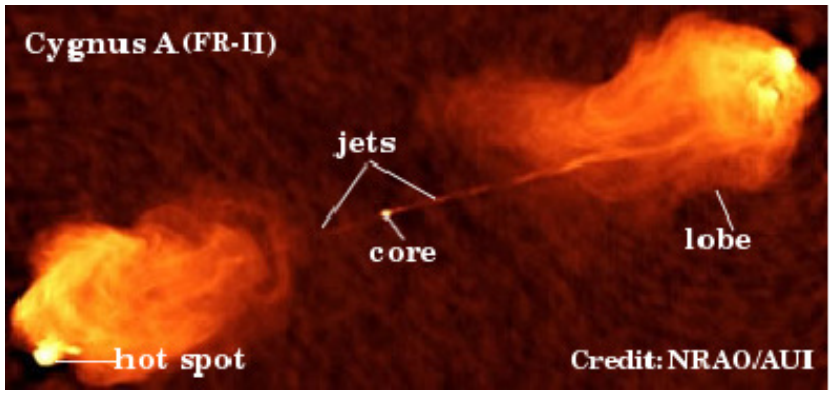

Metrics

- distance between to points in Euclidean space (3D): $(\Delta d)^2 = (\Delta x)^2 + (\Delta y)^2 + (\Delta x)^2$
- Minkovsky metric (special relativity) (4D): $ds^2 = dx_1^2 + dx_2^2 + dx_3^2 - c^2 dt^2$
- Metric in general relativity (4D):
  - consider two events, where the difference in each of their four generalized coordinates $(x^\mu, \mu = 0, 1, 2, 3)$ is an infinitesimal quantity
  - "distance" between these events is given by:
    $$\boxed{ds^2 = g_{\mu\nu} dx^\mu dx^\nu}$$
    $g_{\mu\nu}$ = components of the metric tensor (a 4×4 matrix) (compact writting of the metric tensor, aka, line element)
  - metric tensor at each point of the space-time is covariant, symmetric ($g_{\mu\nu} = g_{\nu\mu}$), and nondegenerate ($\det g_{\mu\nu} \neq 0$), with a signature of either -2 or +2

Space-like and time-like vectors

- for any vector v^μ, the metric assigns the real number $||v||^2 = g_{\mu\nu} v^\mu v^\nu$, where $||v||$ is the norm of the vector
- in GR the space-time is a pseudo-Riemannian manifold, thus:
  vector squared norm can be positive, negative, or null, and consequently, the vector is called time-like, space-like, or null

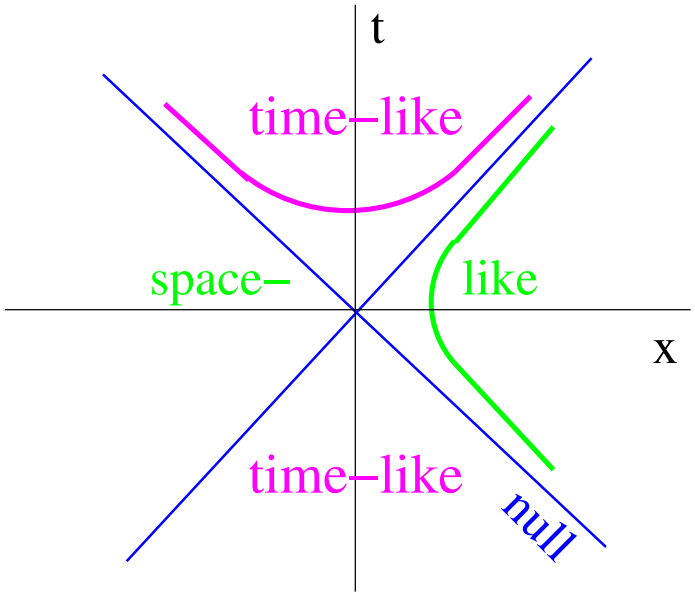

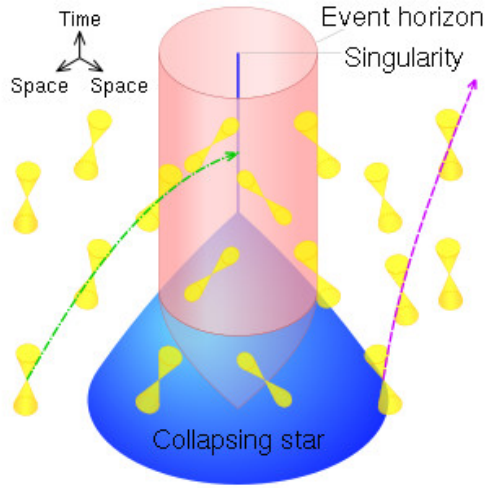

wikipedia

About general relativity

→ Einstein identified the intrinsic property of the spacetime with its geometry

Gravitation ≡ Spacetime geometry

→ in the presence of a source of gravitation, the gravitational effects will not be described through an explicit external force but through the non-Euclidean nature of the spacetime geometry!

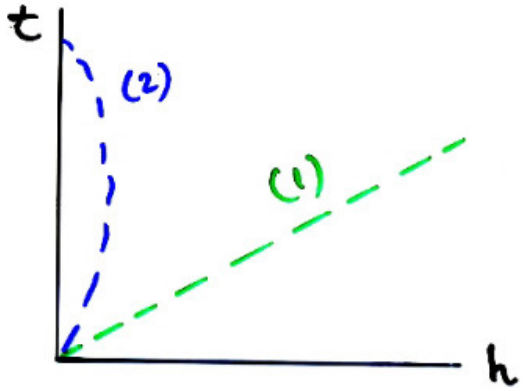

(1) trajectory of a freely moving particle
(2) particle moving under the Earth's gravity
→ in Newtonian gravity, it's the Earth gravitational FORCE which bends the trajectory
→ in Einstein's view the line is also "straight" but the spacetime is NON-EUCLIDEAN because of Earth's gravity

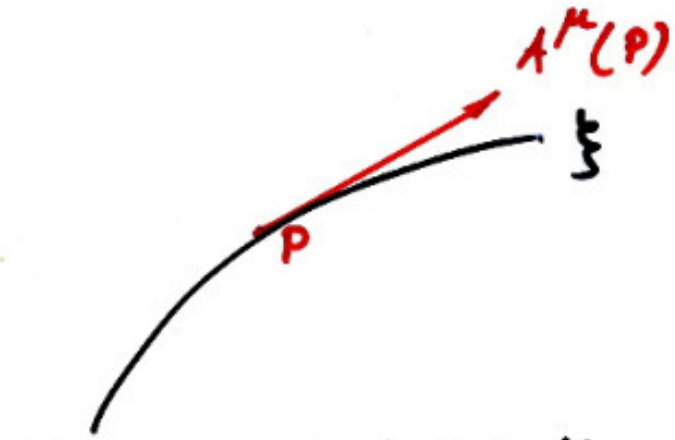

The tangent at P to the curve ξ is a contravar. vector

→ dynamical analogy :

→ velocity (tangent) like vectors = contravariant

→ force (normal) like vectors = covariant

→ rate of work = scalar

- GR is a result of Einstein's attempt to find the relativistic equivalent of Poisson's equation $\boxed{\nabla^2\varphi = -4\pi G\rho}$, where φ is the gravitational potential of a distribution of matter with the density ρ and G is the constant of gravitation
- heuristically, the first step is to replace the mass density with the time-time component of the tensor describing a physical system, in the limit of a weak field
- tensor in question is the stress energy-momentum tensor of the matter: $\boxed{T^{\mu\nu}}$
- second step is to look for a tensor whose components involve the metric tensor and its first and second derivative, assuring a second-order partial differential equation generalizing the Poisson equation, whose divergence vanishes

- quantity which distinguishes between a flat and curved space-time is the Riemann tensor, whose trace is the Ricci tensor $R_{\mu\nu}$
- in covariant form, Einstein's equations are:

$$\boxed{R_{\mu\nu} - \frac{1}{2} g_{\mu\nu} R = \frac{8\pi G}{c^2} T_{\mu\nu}}$$

- left hand side = so-called Einstein tensor $\boxed{G_{\mu\nu}}$, where $R = R^{\mu}_{\mu} = g^{\mu\nu} R_{\mu\nu}$ is the curvature scalar
- Enstein's eq. shows that the gravitational field can be described by a purely geometric quantity, its source being the matter tensor

- in covariant form, Einstein's equations are:

$$\boxed{R_{\mu\nu} - \frac{1}{2} g_{\mu\nu} R = \frac{8\pi G}{c^2} T_{\mu\nu}}$$

- in GR general relativity, there is complete freedom in choosing the coordinate system; i.e., a given space-time can be represented by different coordinates
- even though the metric tensor components depend on the coordinate system, the space-time itself does not
- the physical events happen independently of our observations; it must be possible to express physical laws that take the same form whatever coordinate system one chooses
- thus, the laws are called covariant, and Einstein's principle is the principle of general covariance
- all physical laws that hold in flat space-time can be expressed in terms of vectors and tensors, provided that the derivatives are replaced with the covariant derivative

Schwarzschild solution for non-rotating BH

- first solution of the Einstein's vacuum field equations was found by Schwarzschild (1916)
- assumed that the field outside of a distribution of mass M does not change with time and has a spherical symmetry

$$ds^2 = -\left(1 - \frac{r_s}{r}\right) dt^2 + \left(1 - \frac{r_s}{r}\right)^{-1} dr^2 + r^2 \left(d\theta^2 + \sin^2\theta \, d\phi\right)$$

- $r_s = 2MG/c^2$ is the Schwarzschild radius
- factor $(1 - r_s/r)$ in the second term reflects the curvature of the three-dimensional space-time

Schwarzschild solution for non-rotating BH

- first solution of the Einstein's vacuum ($T_{\mu\nu} = 0$) field equations was found by Schwarzschild (1916)
- assumed that the field outside of a distribution of mass M does not change with time and has a spherical symmetry

$$ds^2 = -\left(1 - \frac{r_s}{r}\right) dt^2 + \left(1 - \frac{r_s}{r}\right)^{-1} dr^2 + r^2 \left(d\theta^2 + \sin^2\theta \, d\phi\right)$$

- rate of the flow of the physical (proper) time, τ, at a given point does not coincide with the t-coordinate. It is specified by $d\tau = \sqrt{-g_{tt}}\, dt$
- far from the gravitational source ($r \to \infty$), $g_{tt} \to 1$ and, therefore, $d\tau = dt$; that is, t is the physical time measured by an observer removed to infinity

Schwarzschild solution for non-rotating BH

- first solution of the Einstein's vacuum field equations was found by Schwarzschild (1916)
- assumed that the field outside of a distribution of mass M does not change with time and has a spherical symmetry

$$ds^2 = -\left(1 - \frac{r_s}{r}\right) dt^2 + \left(1 - \frac{r_s}{r}\right)^{-1} dr^2 + r^2 \left(d\theta^2 + \sin^2\theta \, d\phi\right)$$

- parameterization $t = \text{const}$ for the events means simultaneity in the entire reference frame for the observers being at rest in this frame
- Schwarzschild's solution becomes singular at $r = r_s$ or $r = 0$. On the surface $r = r_s$, the norm of the time-like Killing vector is $g_{tt} = 0$, so that the world lines of the particles becomes null (or light-like)

Kerr black holes in Boyer-Lindquist coordinates

- Kerr space-time symmetries, Killing vectors: $\xi_t = (\partial_t)$, $\xi_\phi = (\partial_\phi)$
- line element: $ds^2 = g_{\mu\nu} dx^\mu dx^\nu$, $\mu = 0, 1, 2, 3$
- in geometric units $G = c = 1$ and metric signature $(-, +, +, +)$
- Kerr (1963) metric in Boyer-Lindquist (1967) coordinates (t, r, θ, ϕ):

$$x = (r^2 + a^2)^{\frac{1}{2}} \sin\theta \cos[\varphi - \tan^{-1}(a/r)],$$

$$y = (r^2 + a^2)^{\frac{1}{2}} \sin\theta \sin[\varphi - \tan^{-1}(a/r)],$$

$$z = r \cos\theta,$$

Kerr black holes in Boyer-Lindquist coordinates

- Kerr space-time symmetries, Killing vectors: $\xi_t = (\partial_t)$, $\xi_\phi = (\partial_\phi)$
- line element: $ds^2 = g_{\mu\nu} dx^\mu dx^\nu$, $\mu = 0, 1, 2, 3$
- in geometric units $G = c = 1$ and metric signature $(-, +, +, +)$
- Kerr (1963) metric in Boyer-Lindquist (1967) coordinates (t, r, θ, ϕ):

$$ds^2 = -\left(1 - \frac{2Mr}{\Sigma}\right) dt^2 - \frac{4Mar\sin^2\theta}{\Sigma} dt d\phi + \frac{\Sigma}{\Delta} dr^2 + \Sigma d\theta^2 + \left(r^2 + a^2 + \frac{2Ma^2 r \sin^2\theta}{\Sigma}\right) \sin^2\theta \, d\phi^2$$

geometrical functions: $\Delta = r^2 - 2Mr + a^2$, $\Sigma = r^2 + a^2 \cos^2$

$a = J/(Mc)$, BH spin

Kerr black holes in Boyer-Lindquist coordinates

- Kerr space-time symmetries, Killing vectors: $\xi_t = (\partial_t)$, $\xi_\phi = (\partial_\phi)$
- line element: $ds^2 = g_{\mu\nu} dx^\mu dx^\nu$, $\mu = 0, 1, 2, 3$
- in geometric units $G = c = 1$ and metric signature $(-, +, +, +)$
- Kerr (1963) metric in Boyer-Lindquist (1967) coordinates (t, r, θ, ϕ):

$$g_{\mu\nu} = \begin{pmatrix} g_{tt} & 0 & 0 & g_{t\phi} \\ 0 & \frac{\Sigma}{\Delta} & 0 & 0 \\ 0 & 0 & \Sigma & 0 \\ g_{t\phi} & 0 & 0 & g_{\phi\phi} \end{pmatrix}$$

geometrical functions: $\Delta = r^2 - 2Mr + a^2$, $\Sigma = r^2 + a^2 \cos^2$

$a = J/(Mc)$, BH spin

- energy-momentum tensor: $T_{\mu\nu}$
- conservation laws: energy: $\mathbf{E} \equiv \mathbf{T} \cdot \partial/\partial t$ and angular momentum: $\mathbf{J} \equiv \mathbf{T} \cdot \partial/\partial \phi$
- event horizon = singularity of the BL coordinates, $\Delta = 0$:

$$r_{\pm} = M \pm \sqrt{M^2 - a^2} = r_{\rm g}(1 \pm \sqrt{1 - a_*})$$

$$r_{\rm g} = GM/c^2 \,\text{gravit. radius}$$

$a_* = a/r_{\rm g}$, $\boxed{-1 \leqslant a_* \leqslant 1}$,
BH spin parameter

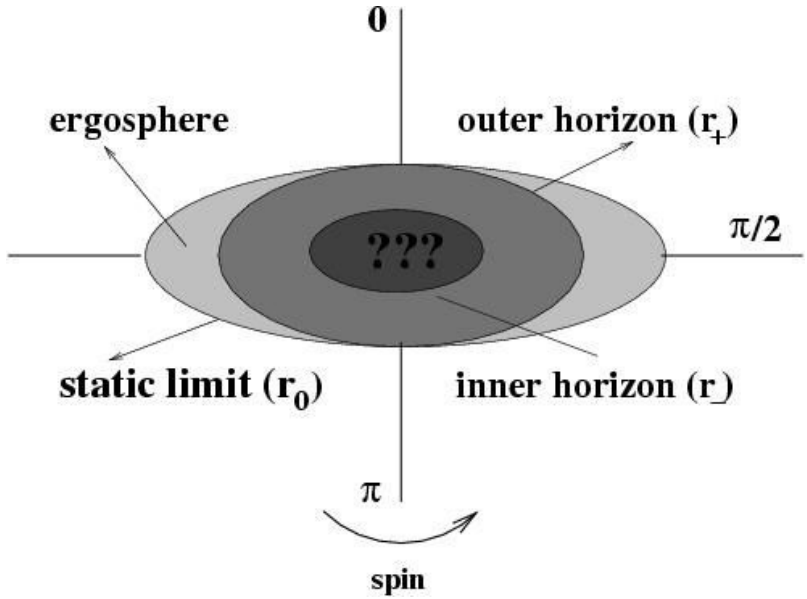

- frame-dragging effect: nothing inside the ergosphere can remain at rest with respect to distant observers, it must co-rotate with the BH rotation
- to study particle motion we need a reference frame which does not rotate: locally non-rotating frame of zero angular momentum observers (ZAMOs)

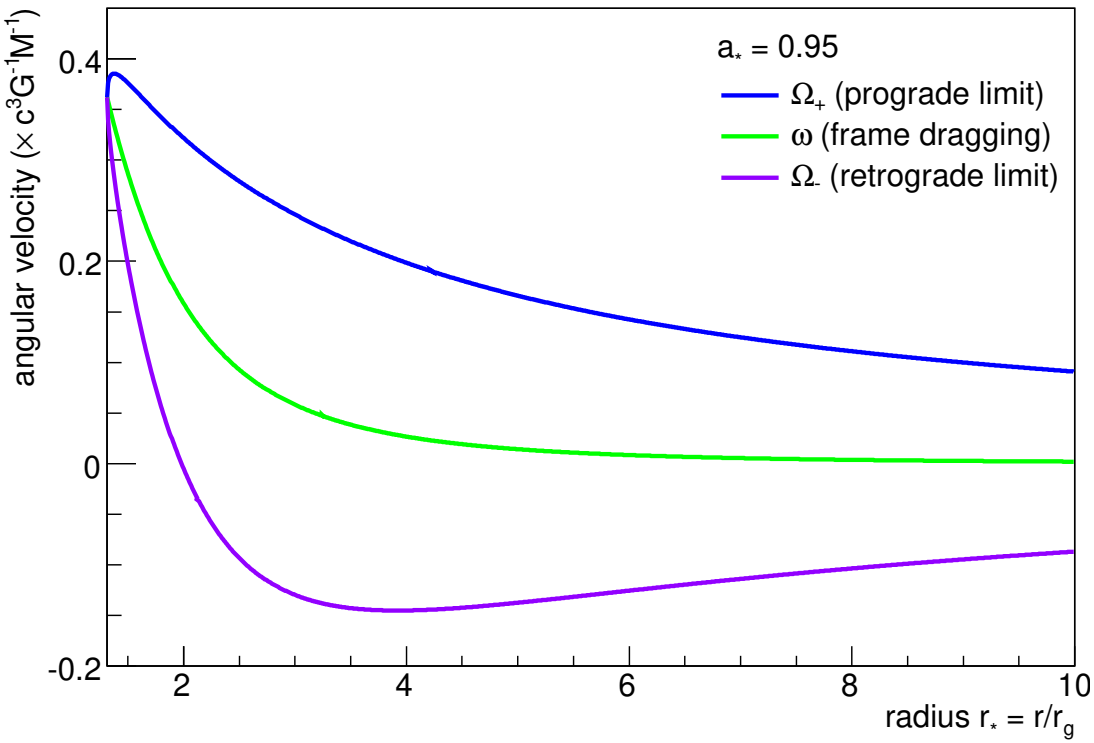

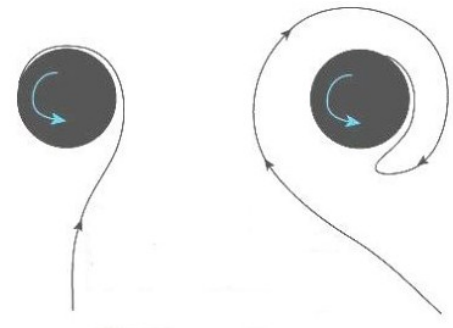

- ergosphere (stationary limit surface): time-like Killing vector becomes null:

$$\xi_t \cdot \xi_t = g_{tt} = 0 \Rightarrow r_{\rm sl} = r_{\rm g}[1 + (1 - a_*^2 \cos^2\theta)^{1/2}]$$

$$(r_{\rm sl})_{\theta=\pi/2} = 2\, r_{\rm g}$$

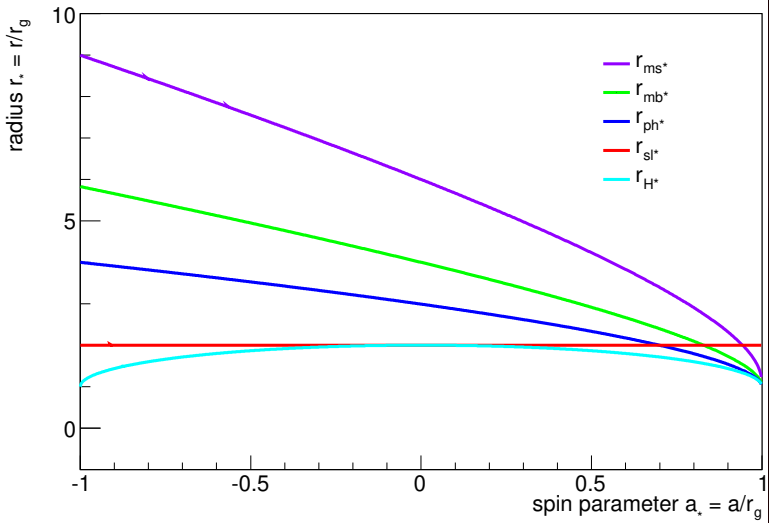

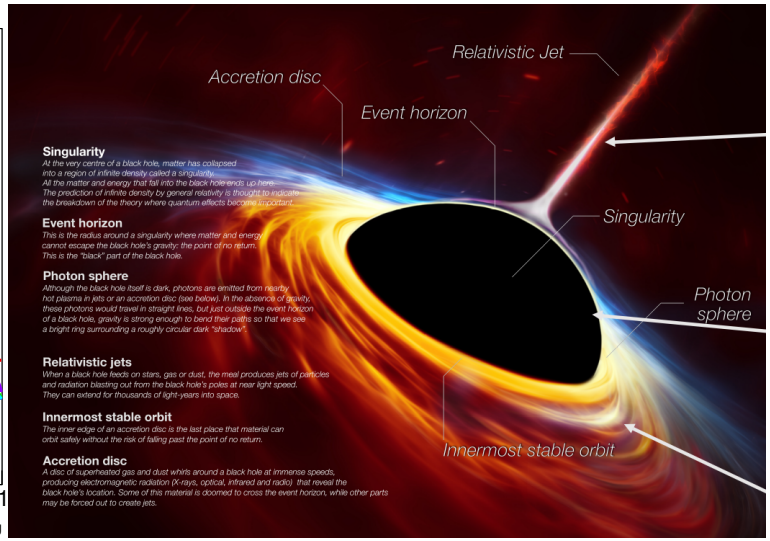

Penrose process (1969)

- Starting from outside of the ergosphere: a particle of energy $E^{(0)}$ splits as it enters the ergosphere of the black hole into a particle with energy $E^{(1)} < 0$ which is captured by the hole, and a second particle with energy $E^{(2)} = E^{(0)} + |E^{(1)}|$ which escapes to infinity (top view)
- energy (mass) extraction 20.7%

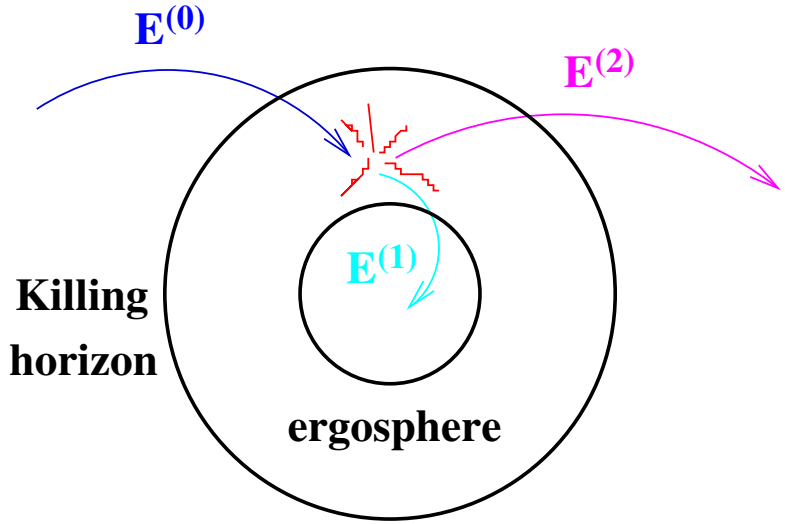

- BH spin-down:

$$\boxed{M^2 = M_{irr}^2 + \frac{J^2}{4M_{irr}^2}}$$

M_{irr} – BH irreducible mass
$\frac{J^2}{4M_{irr}^2}$ – the contribution of the rotational kinetic energy to the square of the inertial mass of the black hole – this rotational energy is being extracted by the Penrose processes

- Bardeen (1972) derived the equations governing the particle trajectory for orbits in the BH equatorial plane
- for circular motion, the particle specific energy and angular momentum are:

$$E^{\dagger} = E/m = \frac{r^{3/2} - 2Mr^{1/2} \pm aM^{1/2}}{r^{3/4}(r^{3/2} - 3Mr^{1/2} \pm 2aM^{1/2})^{1/2}}$$

$$L^{\dagger} = L/m = \frac{\pm M^{1/2}(r^2 \mp 2aM^{1/2}r^{1/2} + a^2)}{r^{3/4}(r^{3/2} - 3Mr^{1/2} \pm 2aM^{1/2})^{1/2}}$$

- particle angular velocity is:

$$\Omega = \frac{d\phi}{dt} = \pm \frac{M^{1/2}}{r^{3/2} \pm M^{1/2}a}$$

- circular orbits do not exist for all radii; the denominator in eqs. for $E^\dagger$ and $L^\dagger$ must have a real value

$$r^{3/2} - 3Mr^{1/2} \pm 2aM^{1/2} \geq 0$$

- Photon orbits: obtained from the limiting condition in eq. above

$$\boxed{r_{\mathrm{ph}*} = 2\left\{1 + \cos\left[2/3\cos^{-1}\left(\mp a_*\right)\right]\right\}}$$

At $r = r_{\mathrm{ph}*}$, $E^\dagger$ becomes infinity, therefore it is a photon orbit

- Marginally bound orbits: an unbound circular orbit is for $E^\dagger > 1$. The marginally bound orbits correspond to $E^\dagger = 1$, for particles falling towards the BH from rest, as seen at infinity,

$$\boxed{r_{\mathrm{mb}*} = 2 \mp a_* + 2\left(1 \mp a_*\right)^{1/2}}.$$

A particle with an orbit $r < r_{\mathrm{mb}}$ falls directly into the BH

- Innermost stable (circular) orbits: Bound circular orbits are not all stable. The condition of stability implies a maximum binding energy of the particles in the BH gravitational potential $(1 - E^{\dagger})$, which gives a minimum particle angular momentum

$$\boxed{r_{ms*} = 3 + z_2 \mp \left[(3 - z_1)(3 + z_1 + 2z_2)\right]^{1/2}}$$

$$z_1 = 1 + \left(1 - a_*^2\right)^{1/3}\left[(1 + a_*)^{1/3} + (1 - a_*)^{1/3}\right]$$

$$z_2 = \left(3a_*^2 + z_1^2\right)^{1/2}$$

- in the theory of thin accretion disks (Novikov & Thorne 1973), the inner edge of the disk is located at the innermost stable radius
- when the disk particles reach this radius, they drop out of the disk and go directly into the BH
- here, BH is represented by the stretched horizon

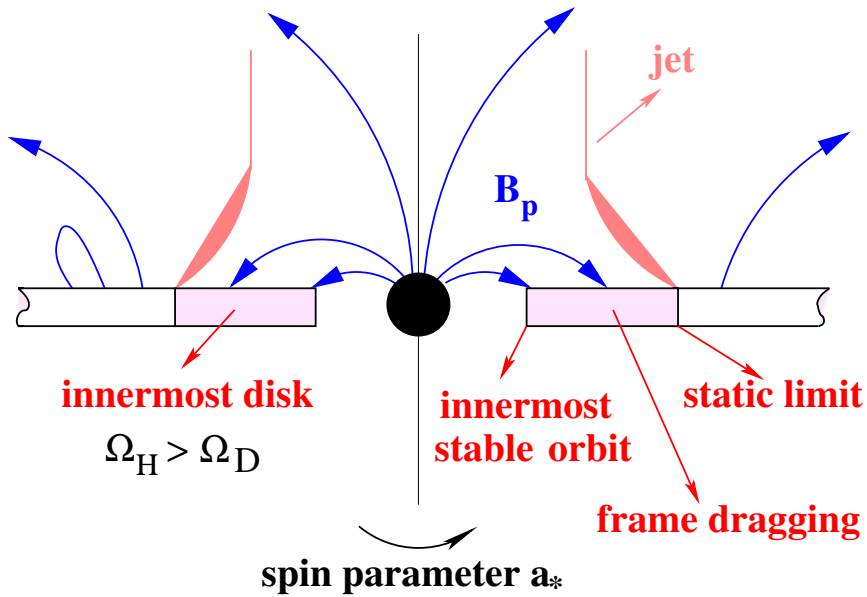

Kerr-Schild solution for rotating black holes

$$
\begin{aligned}
ds^2 = &-\left(1-\frac{2Mr}{\Sigma}\right)dt^2+\left(1+\frac{2Mr}{\Sigma}\right)dr^2+\Sigma d\theta^2\\
&+\left[(r^2+a^2)+\frac{2Mr}{\Sigma}a^2\sin^2\theta\right]\sin^2\theta\, d\phi^2\\
&+\frac{4Mr}{\Sigma}dt\,dr-\frac{4Mra\sin^2\theta}{\Sigma}dt\,d\phi\\
&-2a\sin^2\theta\left(1+\frac{2Mr}{\Sigma}\right)dr\,d\phi
\end{aligned}
$$

unde $\Sigma = r^2 + a^2\cos^2\theta$

Kerr-Schild solution vs Kerr in BL coordinates

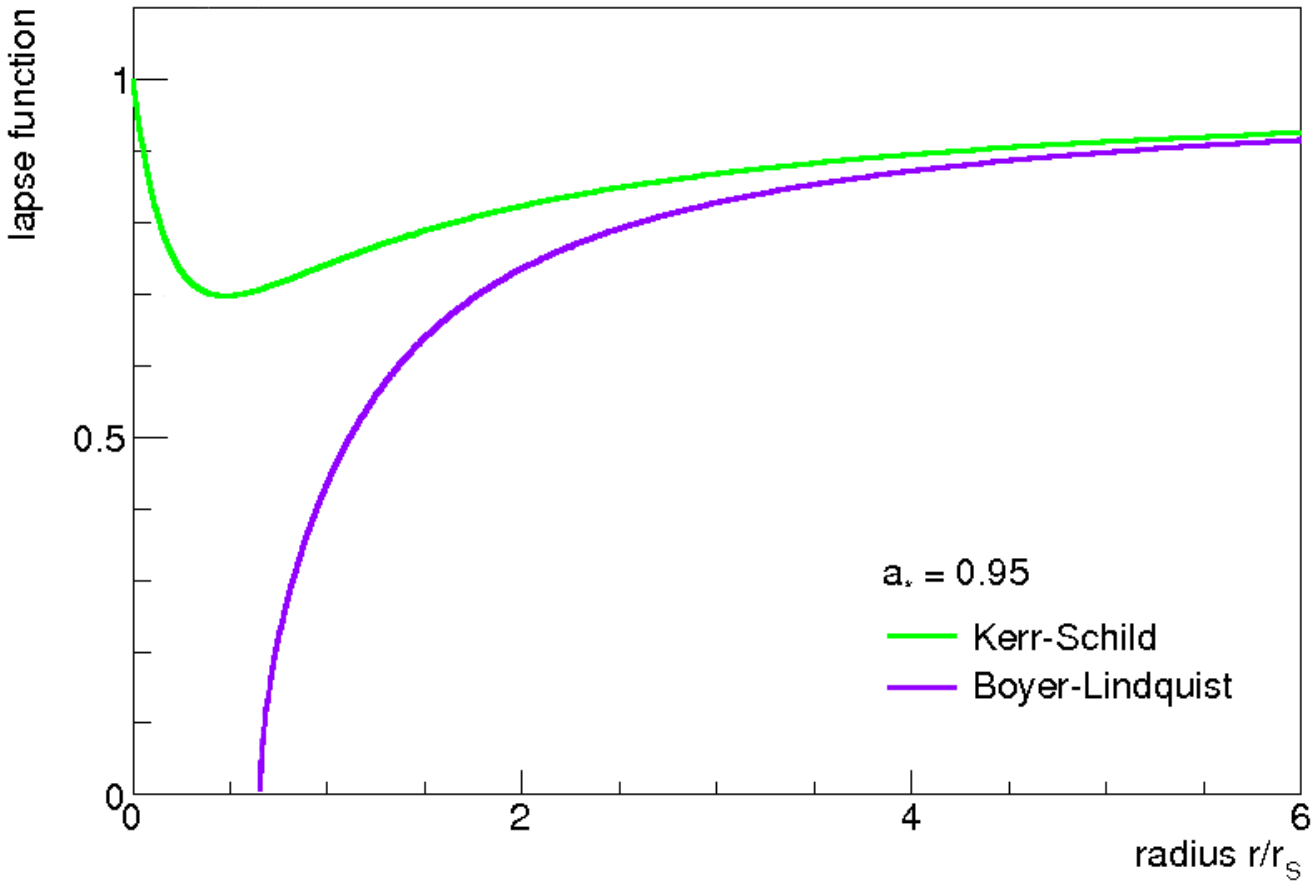

Numerical simulations for rotating black holes

- Einsten's equations do not explicitly describe the time evolution of a system
- to produce numerical solutions of the Einstein equations, the equations are recast into a so-called 3+1 formulation (in which the coordinate time is split from the three spatial coordinates)

$$ds^2 = g_{\mu\nu} dx^\mu dx^\mu = -\alpha^2 dt^2 + \gamma_{ij}(dx^i + \beta^i dt)(dx^j + \beta^j dt)$$

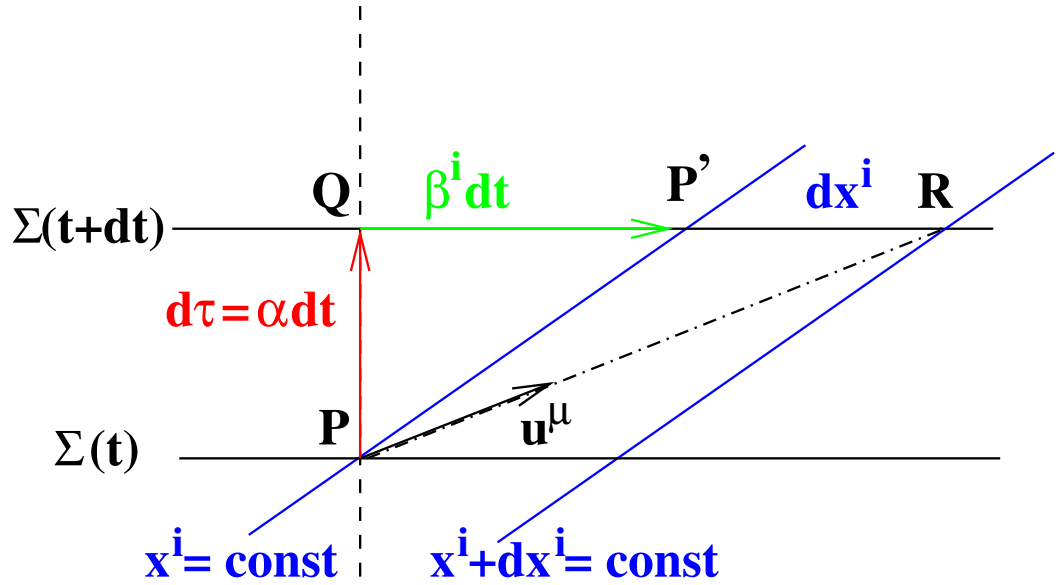

General Relativistic MHD: GRMHD

- 4D stress energy-momentum tensor: $T^{\mu\nu} = T^{\mu\nu}_{\text{fluid}} + T^{\mu\nu}_{\text{EM}}$ $(\mu, \nu = 0, \ldots, 3)$
- Ideal MHD: the fluid is considered to be a perfect conductor (of infinite conductivity)
- GRMHD equations form a set of 8 non-linear hyperbolic PDEs.: conservation of rest mass, conservation of energy and momentum, and evolution of magnetic field (Maxwell's induction equation)
- Plus equation of state for fluid and $\nabla \cdot \mathbf{B} = 0$ condition

In a compact form, the evolution equations of GRMHD can be written as

$$\boxed{\frac{1}{\sqrt{|g|}}\frac{\partial(\sqrt{\gamma}\mathbf{U})}{\partial t}+\frac{1}{\sqrt{|g|}}\frac{\partial(\sqrt{|g|}\mathbf{F})}{\partial x^i}=\mathbf{S}},$$

where the quantities $\mathbf{U}$ (conserved variables), $\mathbf{F}$ (fluxes), and $\mathbf{S}$ (source terms) are

$$\mathbf{U}=\begin{bmatrix} D \\ S_j \\ \tau \\ B^i \end{bmatrix}, \qquad \mathbf{F}=\begin{bmatrix} D\tilde{v}^i \\ T^i_j \\ \alpha T^{ti}-D\tilde{v}^i \\ \tilde{v}^i B^j-\tilde{v}^j B^i \end{bmatrix},$$

$$\mathbf{S}=\begin{bmatrix} 0 \\ T^{\mu\nu}\left(\frac{\partial g_{\nu j}}{\partial x^\mu}-\Gamma^\sigma_{\nu\mu}g_{\sigma j}\right) \\ \alpha\left(T^{\mu t}\frac{\partial \ln\alpha}{\partial x^\mu}-T^{\mu\nu}\Gamma^t_{\nu\mu}\right) \\ 0^i \end{bmatrix}.$$

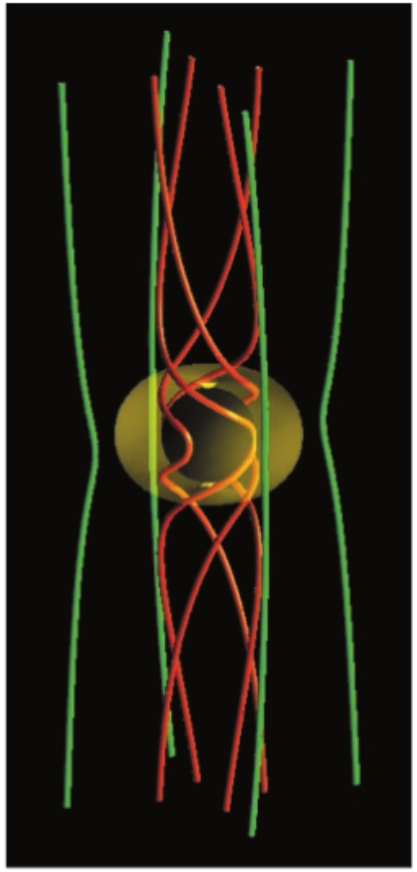

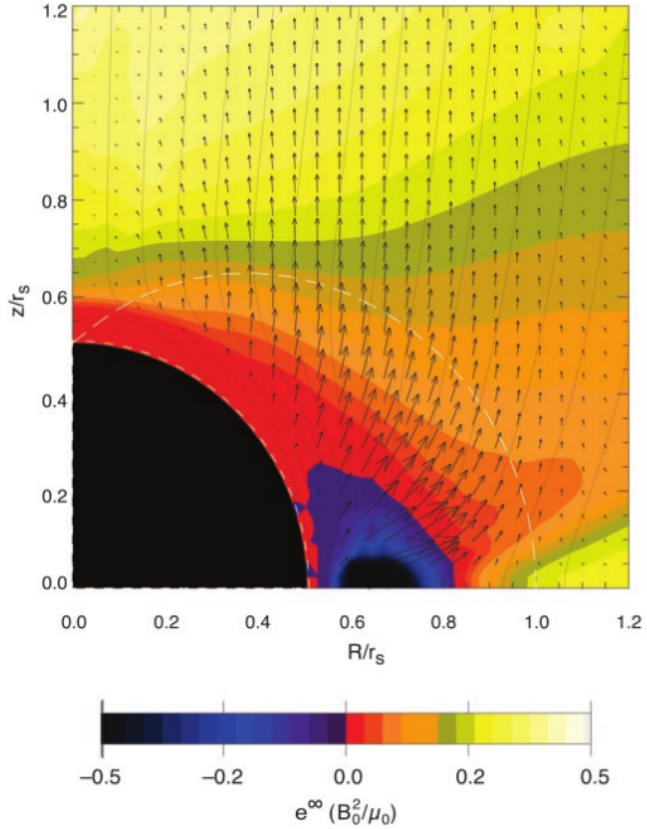

- First GRMHD simulations of jet formation (Koide+ 1998, 2003)
- energy of the spinning BH is extracted magnetically

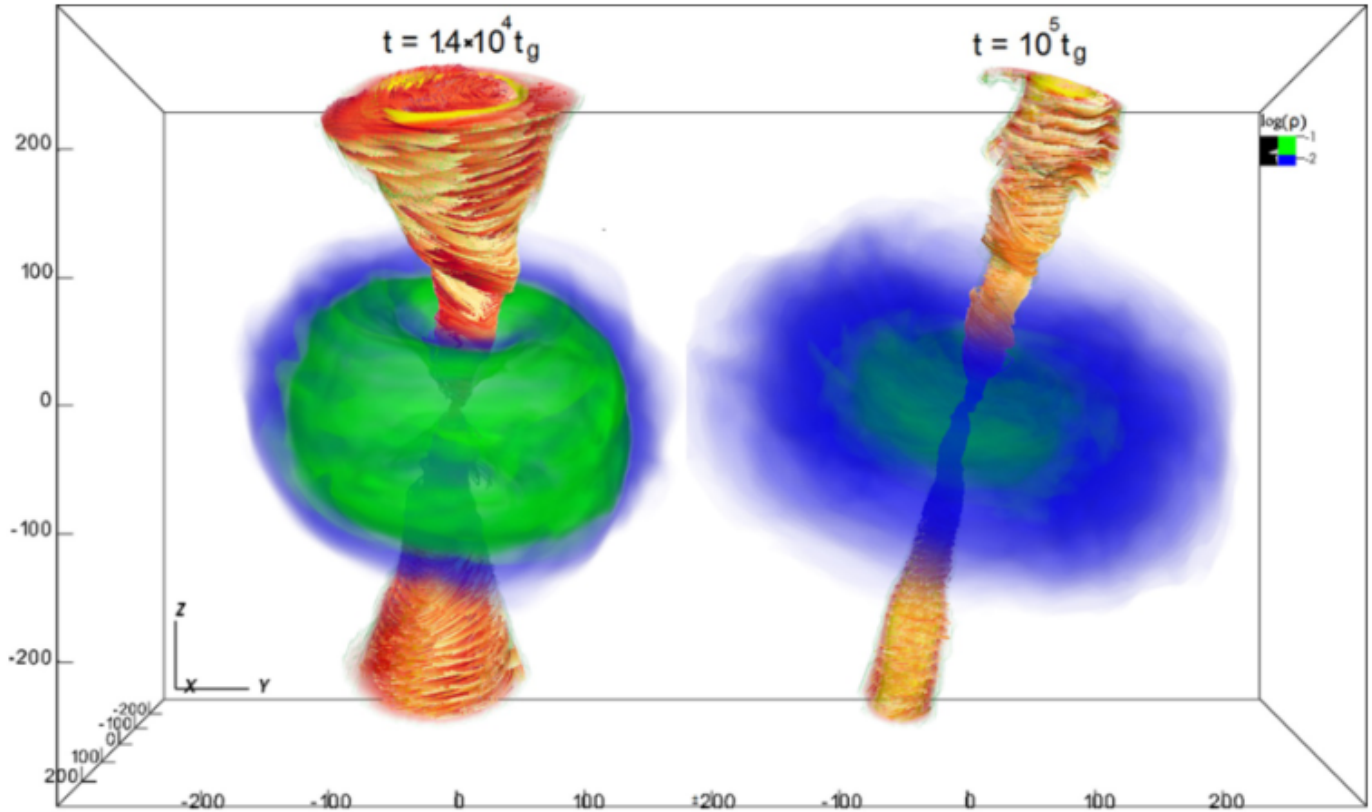

- GRMHD simulations for tilted thin disk simulations; magnetized polar outflows form along the disk rotation axis (Liska+ 2018)

General Relativistic PIC: GRPIC

- GRPIC simulations of jet formation (Watson+Nishikawa 2010)
- tensor form of the Maxwell and Newton-Lorentz equations with Kerr-Schild solution

$$
\begin{aligned}
F^{\alpha\beta}_{;\beta} &= \frac{4\pi}{c} J^{\alpha} \\
F_{\alpha\beta;\gamma} + F_{\beta\gamma;\alpha} + F_{\gamma\alpha;\beta} &= 0 \\
m\left(\frac{du^{\alpha}}{d\tau} + \Gamma^{\alpha}_{rs}\frac{dx^{r}}{d\tau}\frac{dx^{s}}{d\tau}\right) &= qF^{\alpha}_{\beta}u^{\beta}
\end{aligned}
$$

$$
F^{\alpha\beta} = \begin{pmatrix} 0 & B^z & -B^y & -E^x \\ -B^z & 0 & B^x & -E^y \\ B^y & -B^x & 0 & -E^z \\ E^x & E^y & E^z & 0 \end{pmatrix}
$$

The Maxwell tensor field components on a Yee lattice; they are defined on the face and edge of the computational cube

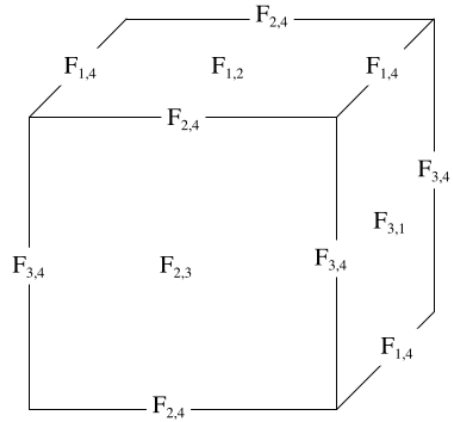

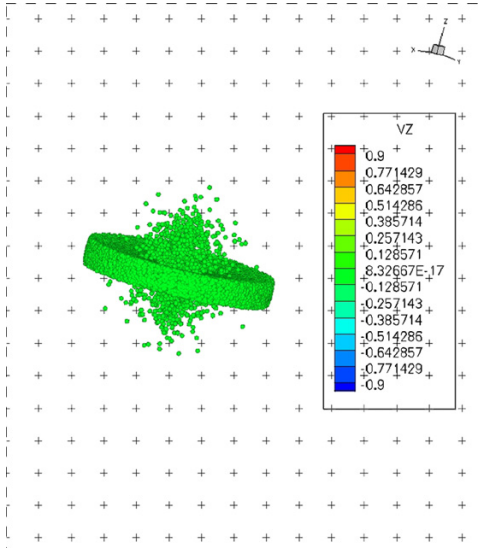

(a) Initial disk and corona

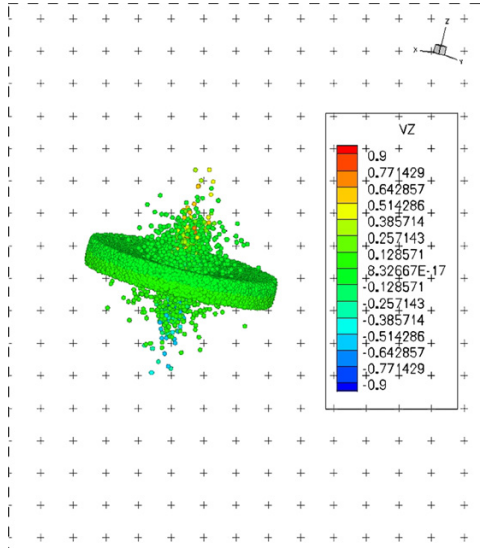

(b) Beginning jet formation

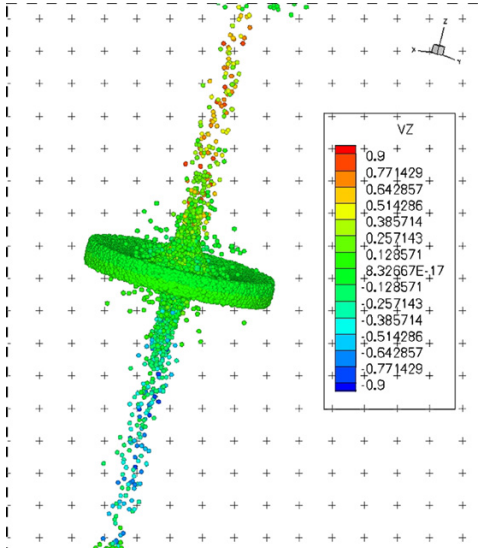

(c) Fast spiraling jet

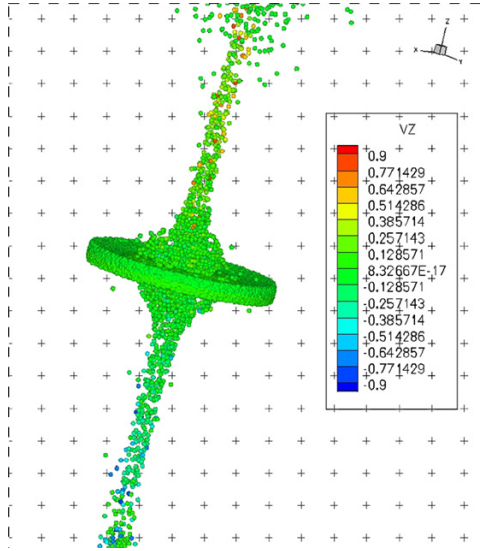

(d) Development of slow moving outside particles surrounding faster particles at the core

Key points

- calculate spectra self-consistently, in the sense that the spectra should be obtained by tracing particles directly from PIC simulations without making assumptions about the magnetic field, particle orbit, and so forth, and by solving the Maxwell equations at the same time
- spectra from electrons accelerated in a cylindrical relativistic jet injected into an ambient plasma at rest
- how does an initially applied toroidal magnetic field affect the growth of plasma instabilities $\rightarrow$ particle acceleration $\rightarrow$ emission of electromagnetic radiation

Radiation from relativistic jets using PIC

- fields are discretized on a finite 3D mesh (Yee lattice): electric fields on cell edges, magnetic fields on cell faces; maintains $\nabla \cdot \mathbf{B} = 0$; 2nd-order accurate in space
- interpolate fields at particle position
- these fields are used to advance particle velocity in time via Lorentz force; leapfrog: 2nd-order accurate in time
- charges and currents are then used as source terms to recalculate fields

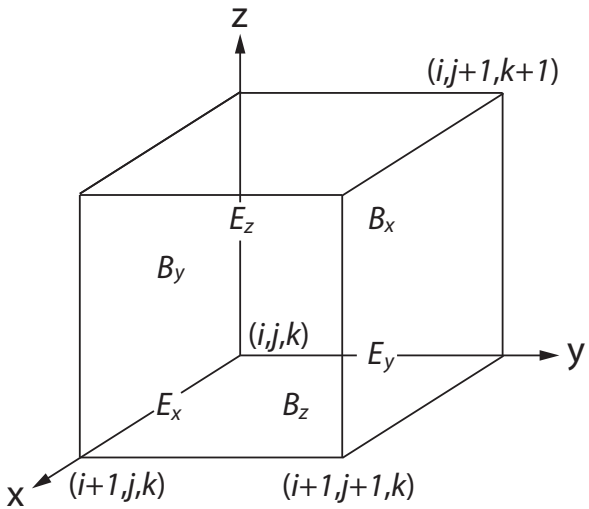

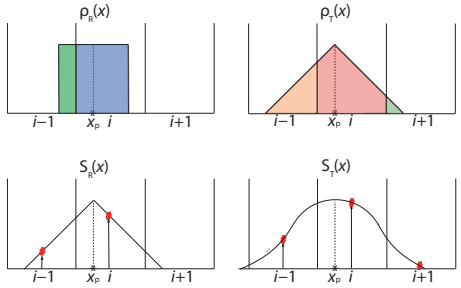

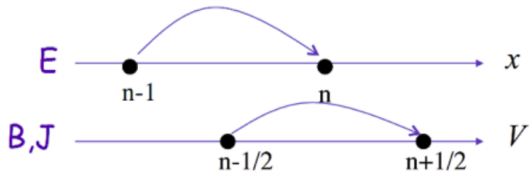

$$\partial_t B = -\nabla \times E,$$
$$\partial_t E = \nabla \times B - J$$

- large scale simulations with $r_{\rm jt} = 100\Delta$ (Meli+ 2023)
- setting: $\Gamma = 15, 100$ and $B_0 = 0.5, 0.1$
- method based on calculated the retarded potentials

  (Hededal 2005, Nishikawa+ 2009)

$$\frac{d^2W}{d\Omega d\omega} = \frac{\mu_0 c q^2}{16\pi^3} \left| \int_{-\infty}^{\infty} \frac{\mathbf{n} \times [(\mathbf{n} - \beta) \times \dot{\beta}]}{(1 - \beta \cdot \mathbf{n})^2} e^{\frac{i\omega(t' - \mathbf{n}\cdot\mathbf{r}_0(t'))}{c}} dt' \right|^2$$

- select about 10000 jet electrons and follow them for 15000 steps ($\Delta t = 0.005\ \omega_{\rm pe}^{-1}$) for about $x = 25\Delta$

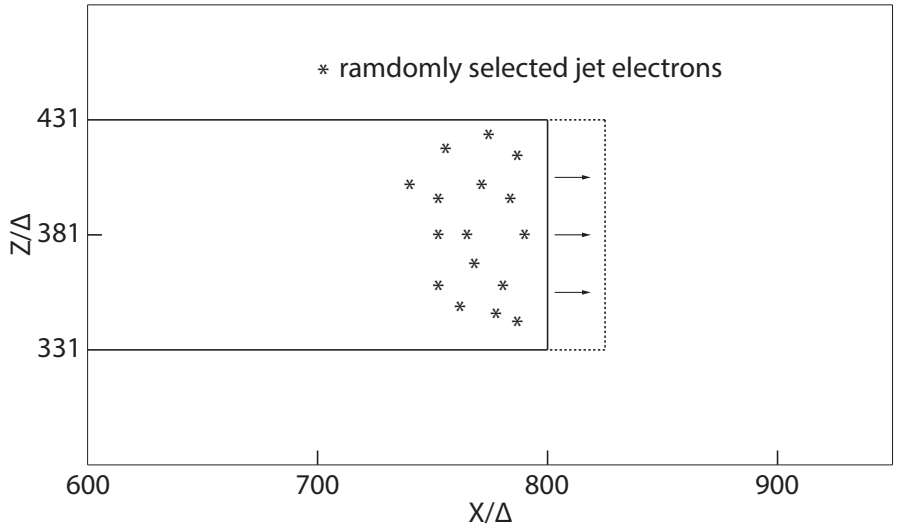

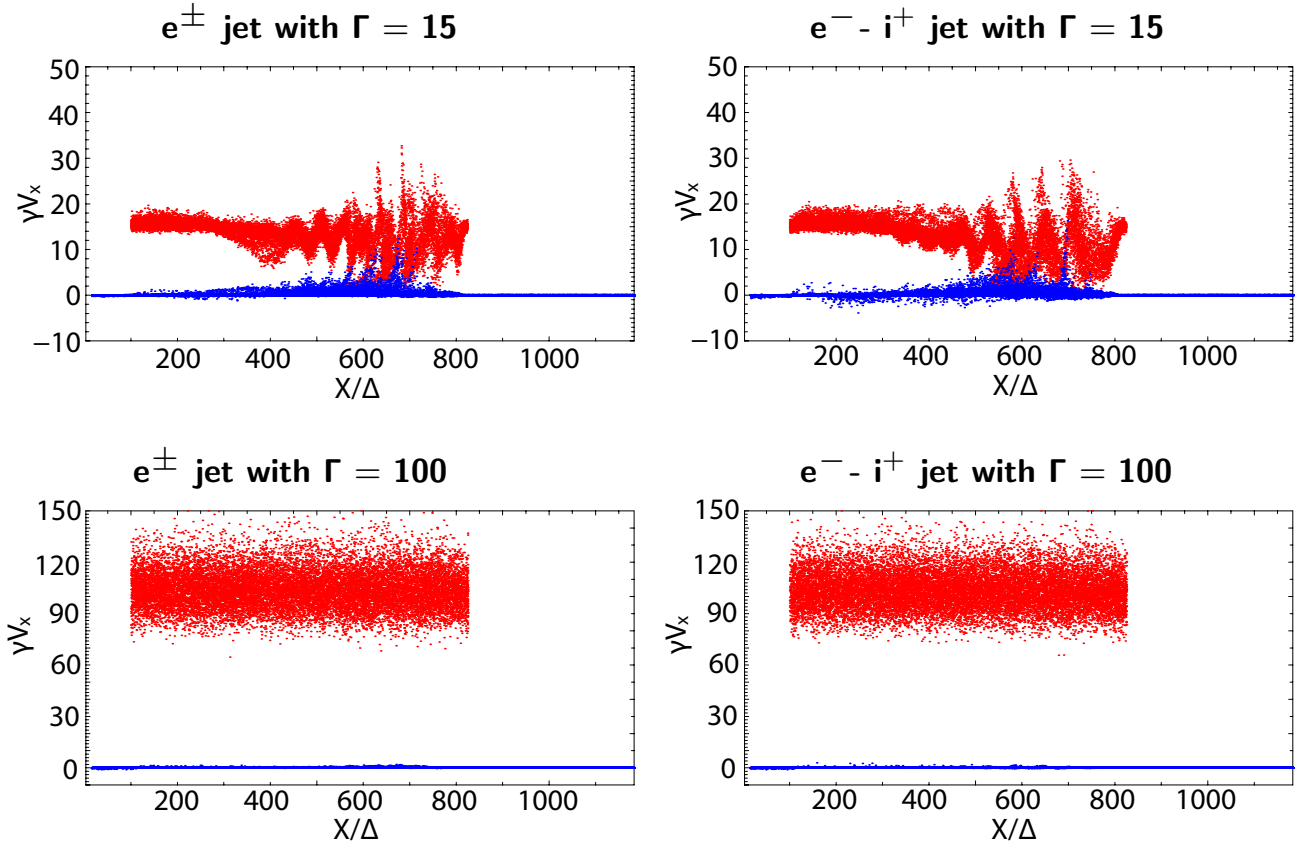

- x - γv_{x} distribution of jet (red) and ambient (blue) electrons for jets with $B_0 = 0.5$, at $t = 725\omega_{\mathrm{pe}}^{-1}$

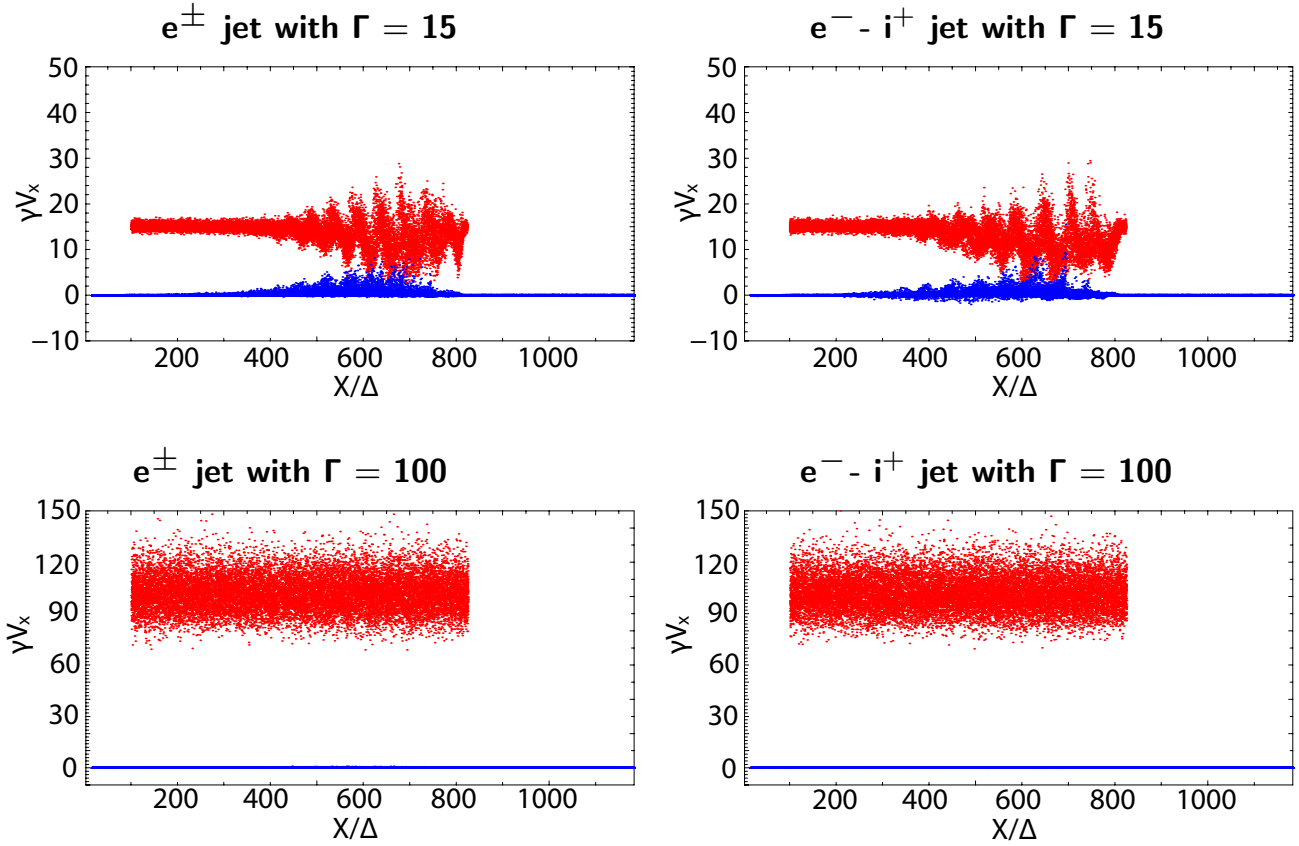

- x - γv_{x} distribution of jet (red) and ambient (blue) electrons for jets with $B_0 = 0.1$, at $t = 725\omega_{\mathrm{pe}}^{-1}$

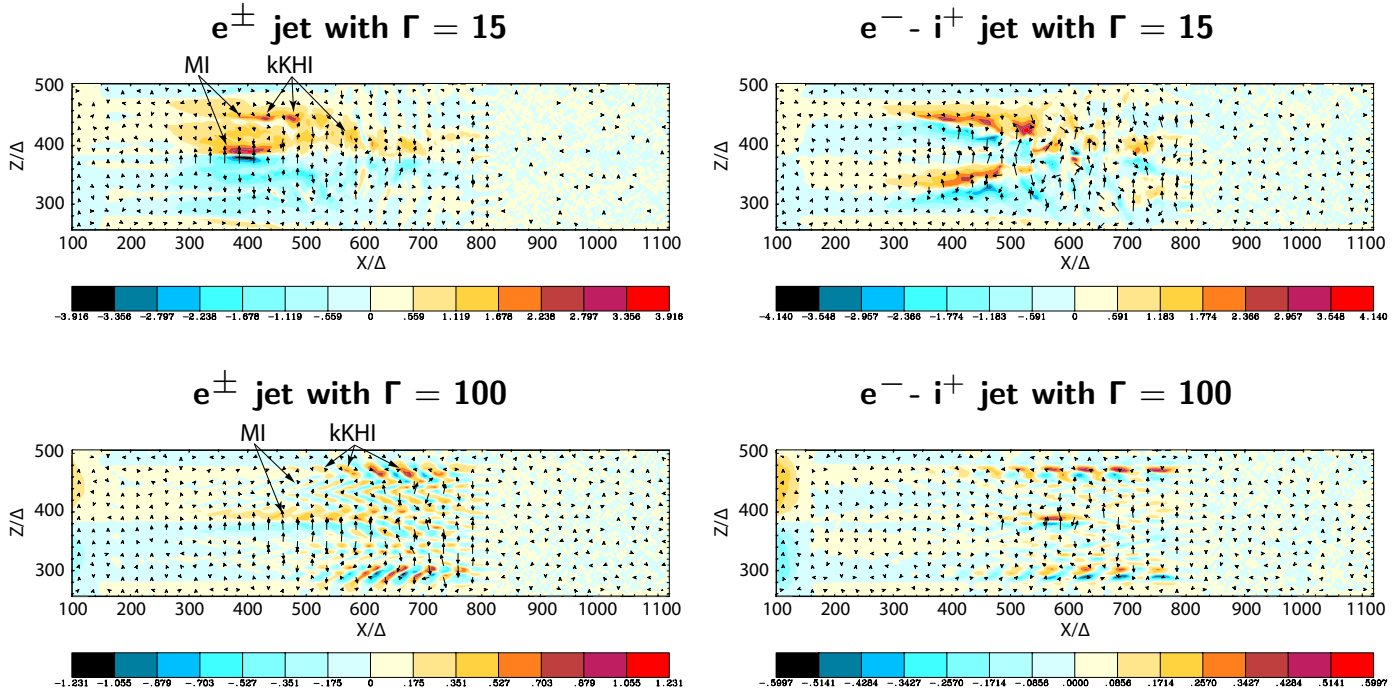

- Color maps of the B_y magnetic field with arrows depicting the magnetic field components in the $x - z$ plane for jets with $B_0 = 0.5$, at $t = 725\omega_{\rm pe}^{-1}$
- maximum and minimum are (a): ± 3.916, (b): ± 4.140, (c): ± 1.231, and (d): ± 0.5997

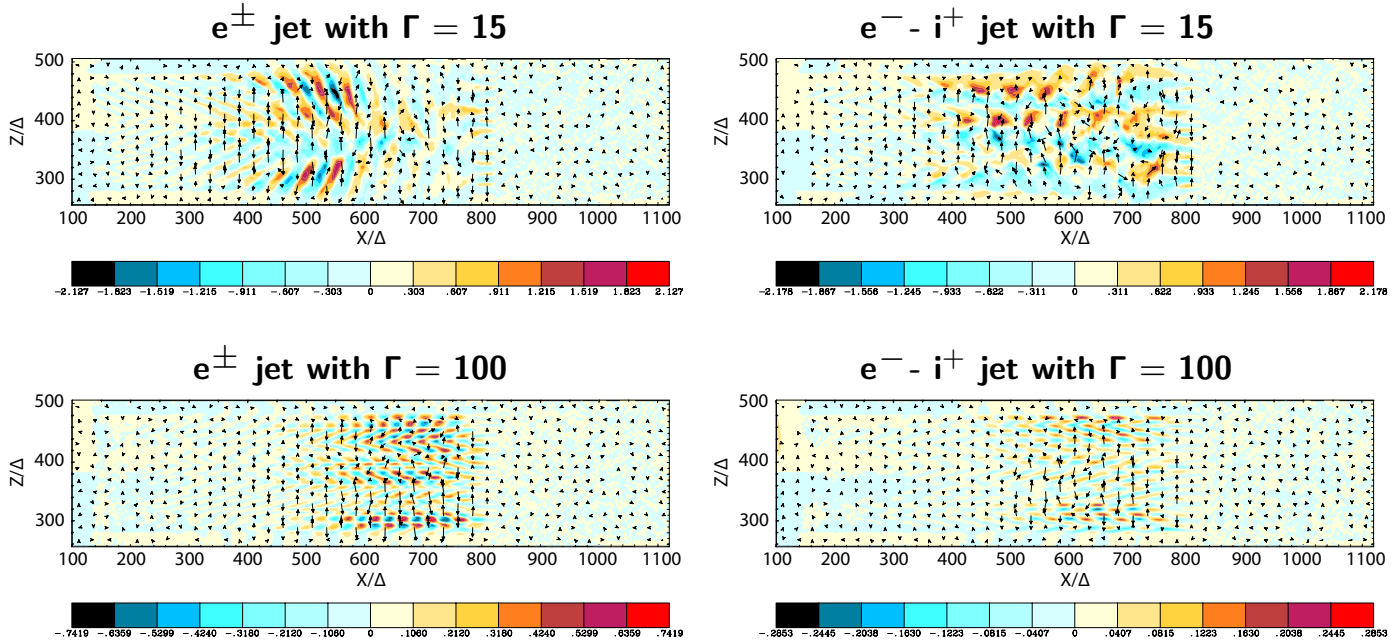

- color maps of the B_y magnetic field with arrows depicting the magnetic field components in the $x - z$ plane for jets with $B_0 = 0.1$, at $t = 725\omega_{\rm pe}^{-1}$
- maximum and minimum are (a): ± 2.127, (b): ± 2.178, (c): ± 0.7419, and (d): ± 0.2853

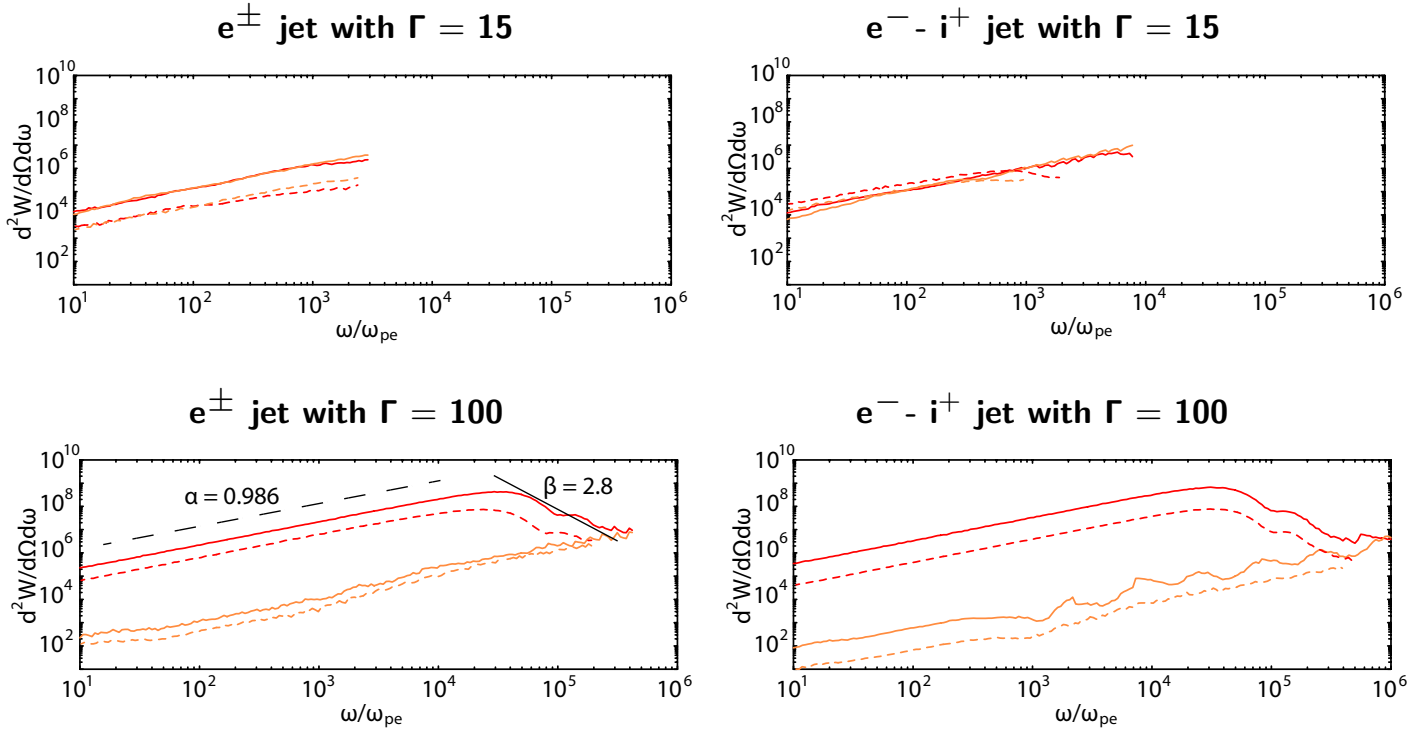

- synthetic spectra for $e^{\pm}$ jets (left panels) and for e^{-}- i^{+} jets (right panels).
- continuous line: $B_0 = 0.5$ and dashed lines: $B_0 = 0.1$
- red lines: spectra for a head-on emission of jet electrons; orange lines: 5°-off emission of radiation

Radiation from relativistic jets using PIC

- fields are discretized on a finite 3D mesh (Yee lattice): electric fields on cell edges, magnetic fields on cell faces; maintains $\nabla \cdot \mathbf{B} = 0$; 2nd-order accurate in space
- interpolate fields at particle position
- these fields are used to advance particle velocity in time via Lorentz force; leapfrog: 2nd-order accurate in time
- charges and currents are then used as source terms to recalculate fields

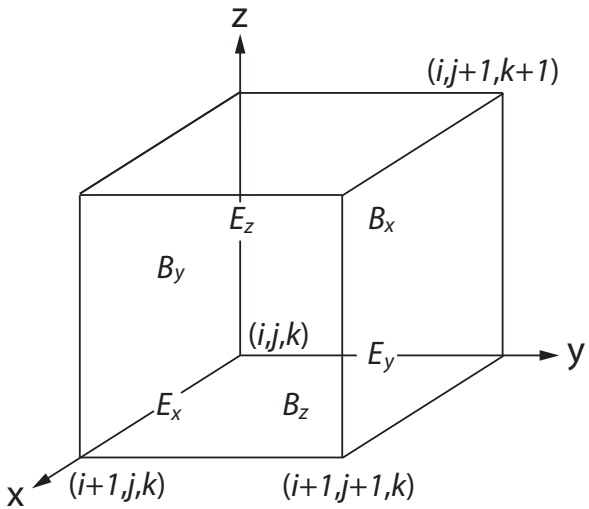

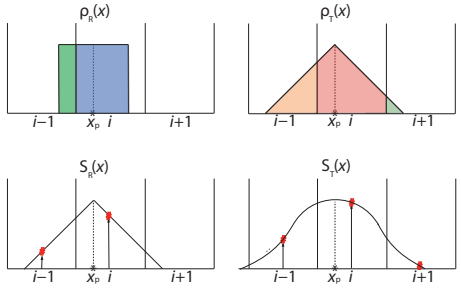

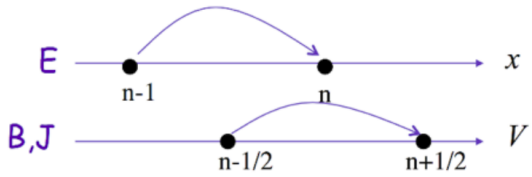

$$\partial_t B = -\nabla \times E,$$
$$\partial_t E = \nabla \times B - J$$

- large scale simulations with $r_{\rm jt} = 100\Delta$ (Meli+ 2023)
- setting: $\Gamma = 15, 100$ and $B_0 = 0.5, 0.1$
- method based on calculated the retarded potentials

  (Hededal 2005, Nishikawa+ 2009)

$$\frac{d^2W}{d\Omega d\omega} = \frac{\mu_0 c q^2}{16\pi^3} \left| \int_{-\infty}^{\infty} \frac{\mathbf{n} \times [(\mathbf{n} - \beta) \times \dot{\beta}]}{(1 - \beta \cdot \mathbf{n})^2} e^{\frac{i\omega(t' - \mathbf{n}\cdot\mathbf{r}_0(t'))}{c}} dt' \right|^2$$

- select about 10000 jet electrons and follow them for 15000 steps ($\Delta t = 0.005\ \omega_{\rm pe}^{-1}$) for about $x = 25\Delta$

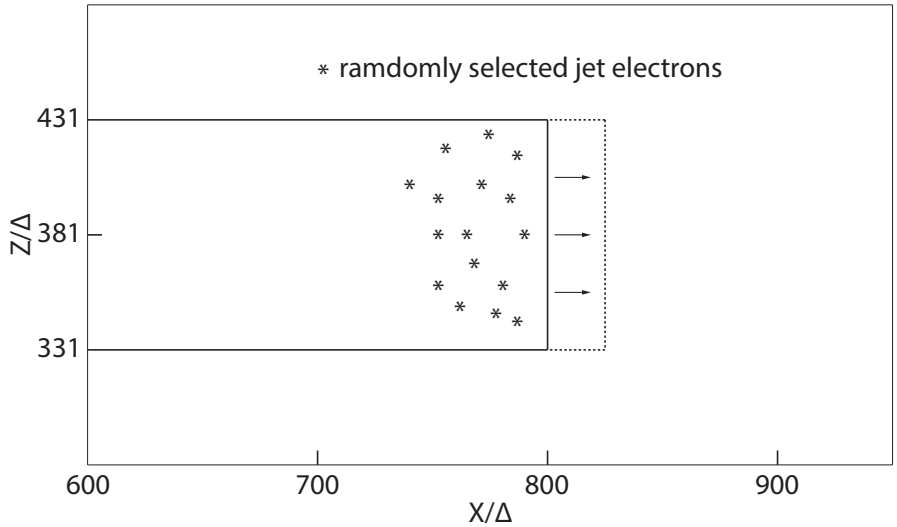

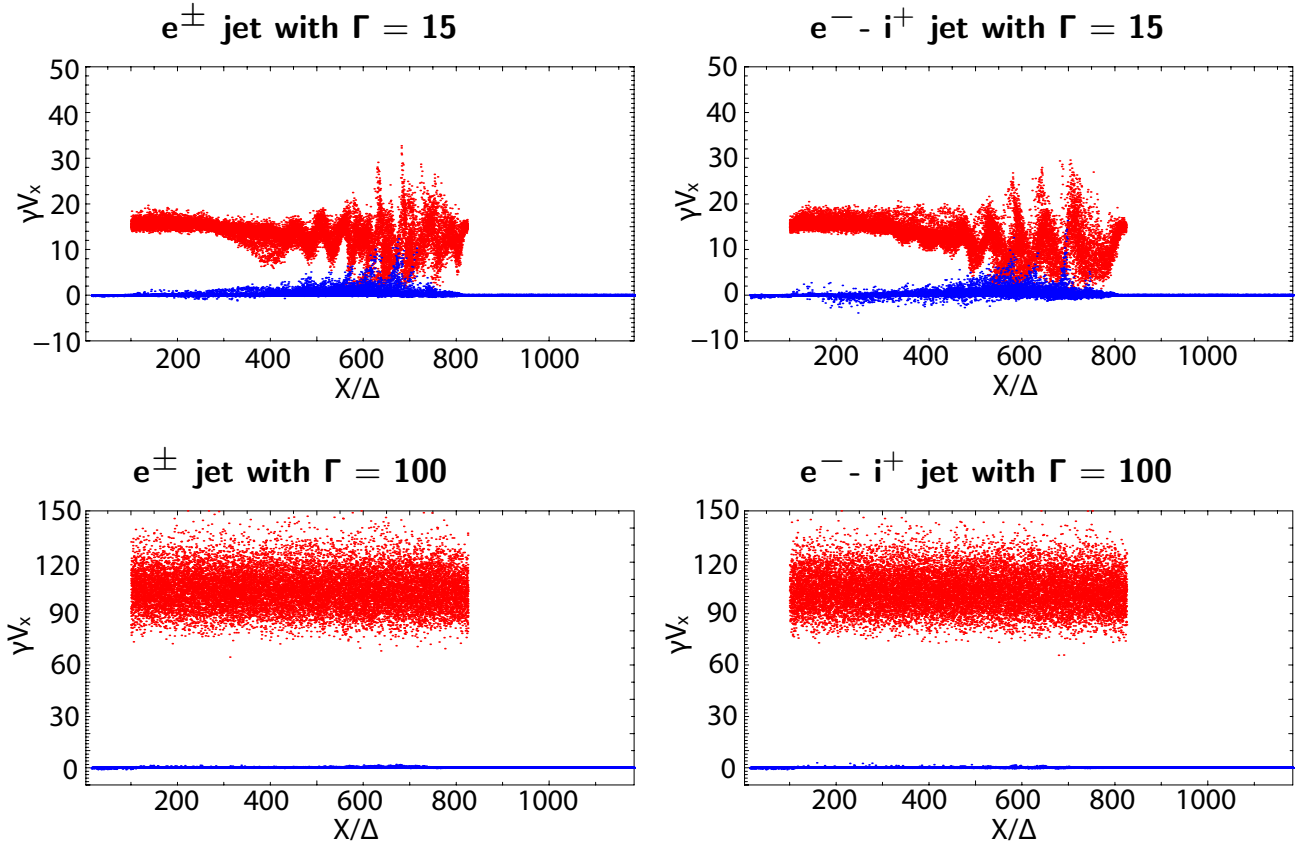

- x - γv_{x} distribution of jet (red) and ambient (blue) electrons for jets with $B_0 = 0.5$, at $t = 725\omega_{\mathrm{pe}}^{-1}$

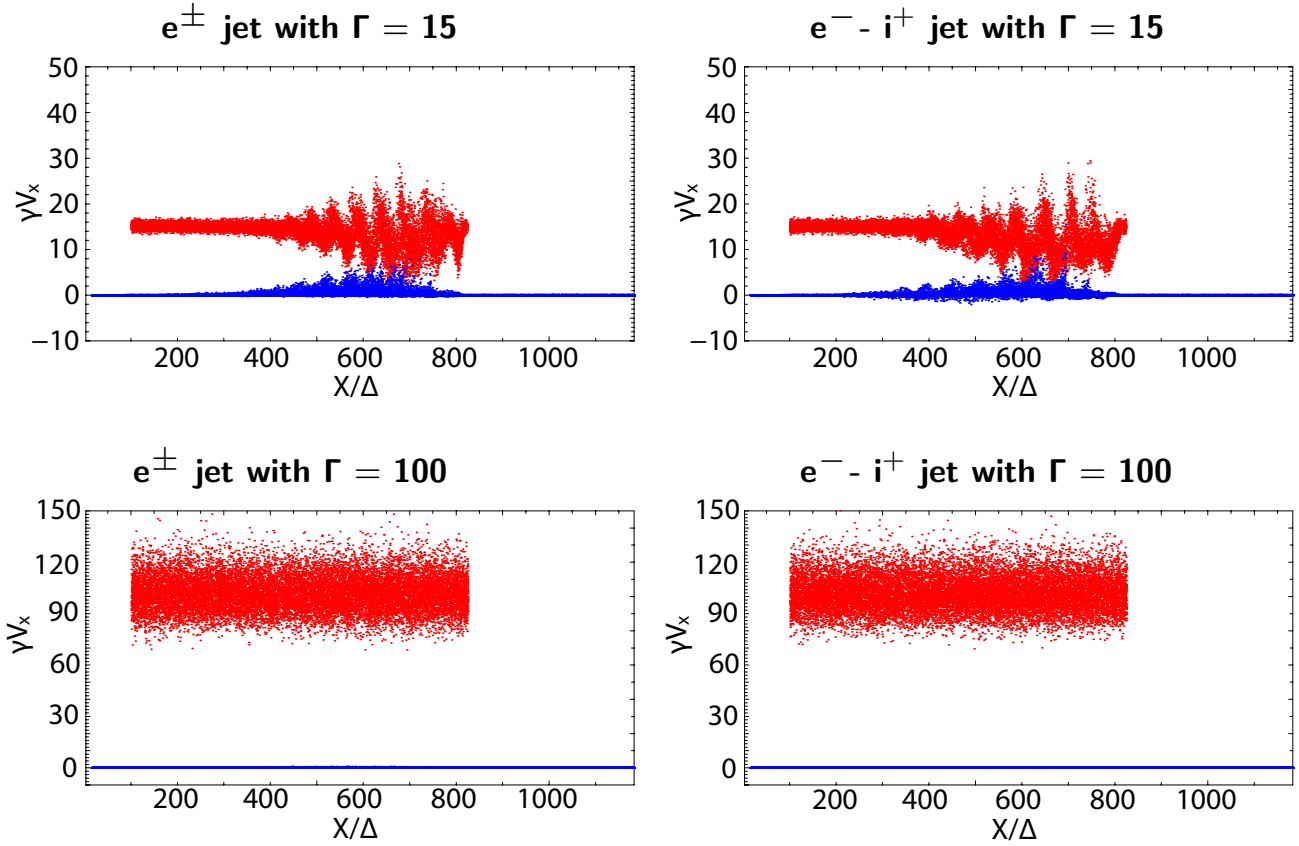

- x - γv_{x} distribution of jet (red) and ambient (blue) electrons for jets with $B_0 = 0.1$, at $t = 725\omega_{\mathrm{pe}}^{-1}$

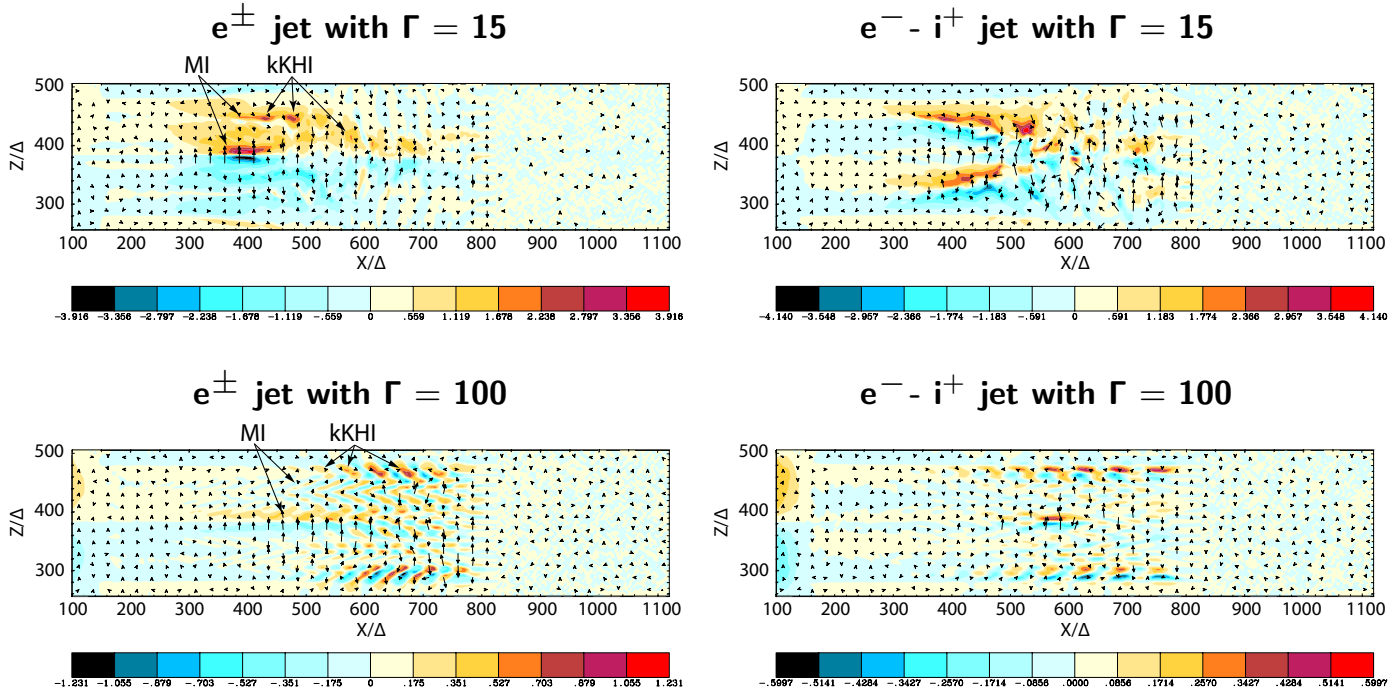

- Color maps of the B_y magnetic field with arrows depicting the magnetic field components in the $x - z$ plane for jets with $B_0 = 0.5$, at $t = 725\omega_{\rm pe}^{-1}$
- maximum and minimum are (a): ± 3.916, (b): ± 4.140, (c): ± 1.231, and (d): ± 0.5997

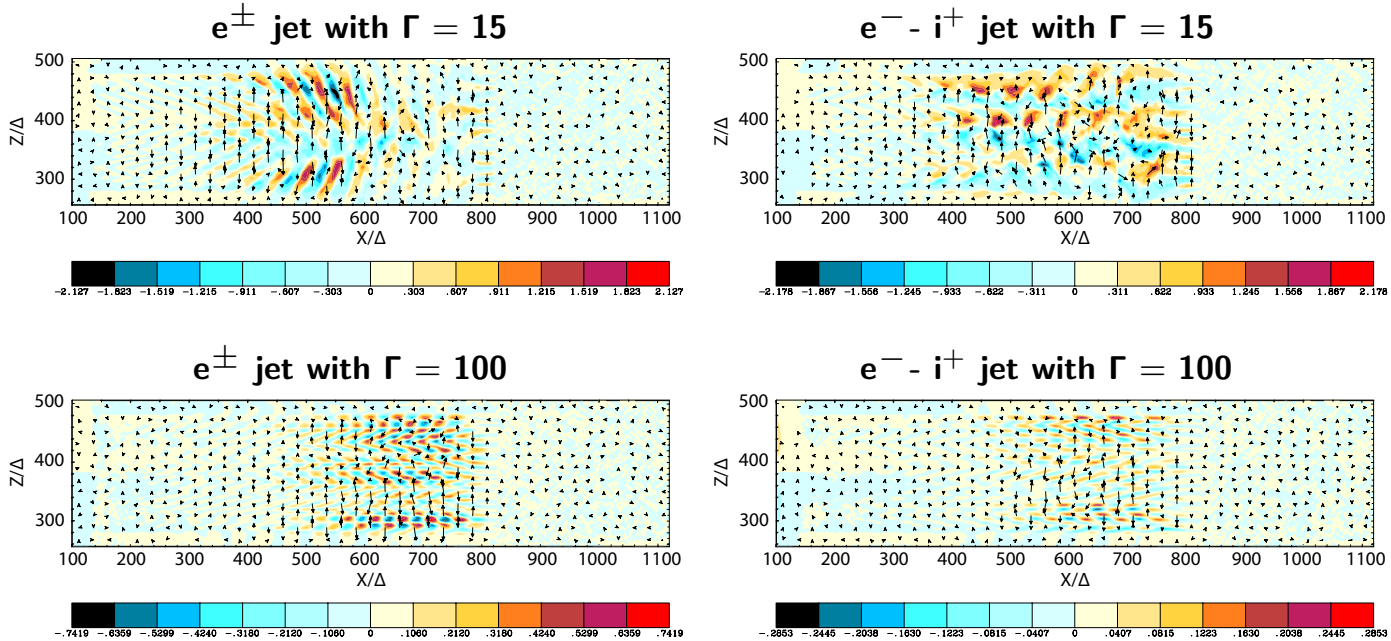

- color maps of the B_y magnetic field with arrows depicting the magnetic field components in the $x - z$ plane for jets with $B_0 = 0.1$, at $t = 725\omega_{\rm pe}^{-1}$
- maximum and minimum are (a): ± 2.127, (b): ± 2.178, (c): ± 0.7419, and (d): ± 0.2853

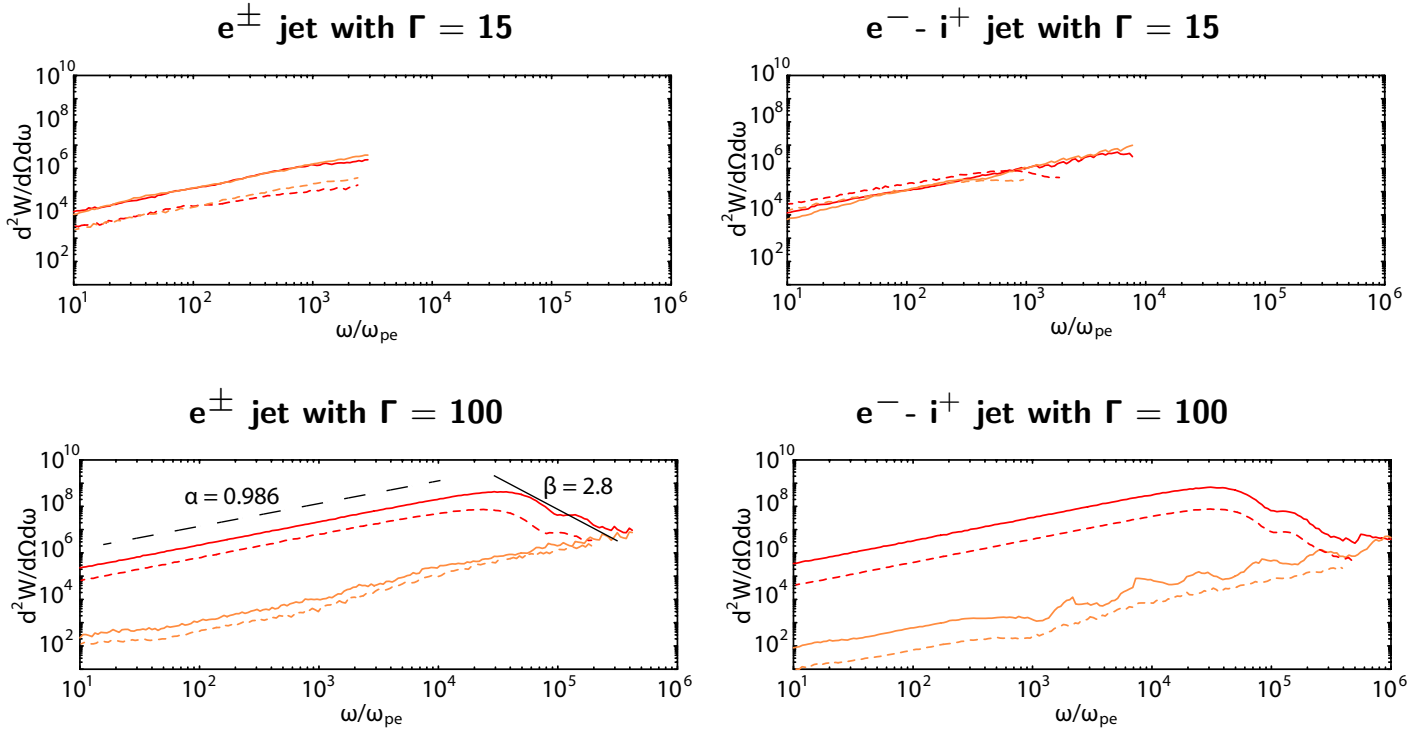

- synthetic spectra for $e^{\pm}$ jets (left panels) and for e^{-}- i^{+} jets (right panels).
- continuous line: $B_0 = 0.5$ and dashed lines: $B_0 = 0.1$
- red lines: spectra for a head-on emission of jet electrons; orange lines: 5°-off emission of radiation

Conclusions

- self-consistently calculate the spectra from PIC simulations
- presence of helical fields suppresses the growth of the kinetic instabilities, such as the Weibel instability, and later on MI and kKHI
- further calculations for different setup of the simulations, e.g., different particle distribution at the injection, plasma quantities, larger simulation grids
- need of allocation for run time of very large PIC simulations, also on Texascale Days at Frontera, TACC